Preparation and Properties of $(C_4H_9NH_3)_2EuI_4$: A Luminescent Organic−Inorganic Perovskite with a Divalent Rare-Earth Metal Halide Framework

David B. Mitzi* and Kangning Liang

IBM T. J. Watson Research Center, P.O. Box 218, Yorktown Heights, New York 10598

Received May 9, 1997[⊗]

$(C_4H_9NH_3)_2EuI_4$ has been prepared through the low-temperature solid-state reaction between $C_4H_9NH_2$·HI and EuI_2, providing the first example of a layered organic−inorganic perovskite with a divalent rare-earth metal in the perovskite sheets. The orthorhombic lattice parameters for the new compound, $a = 8.913(3)$ Å, $b = 8.759(3)$ Å, and $c = 27.793(6)$ Å, refined from powder X-ray diffraction data, are similar to those previously observed for the family $(C_4H_9NH_3)_2MI_4$ (M = Ge, Sn, Pb). The measured europium paramagnetic moment, 7.8(1) μ_b, is consistent with the expected $^8S_{7/2}$ ground state for nominally isolated divalent europium ions. There is no evidence for magnetic ordering of these ions over the temperature range 1.8−300 K. Strong blue photoluminescence is observed at 460(1) nm, a wavelength that is red-shifted approximately 10 nm relative to that for the more three-dimensional perovskite structures $CsEuI_3$ and $CH_3NH_3EuI_3$. Thermal analysis indicates that, in an inert atmosphere, $(C_4H_9NH_3)_2EuI_4$ undergoes bulk decomposition at temperatures above 290 °C.

Introduction

There are currently two classes of the organic−inorganic perovskites, A_2MX_4, where A = organic cation and X = halogen, based on the divalent metal "M" in the inorganic component of the structure. Compounds with transition-metal atoms occupying the "M" site have been studied for a number of years, primarily for the interesting magnetic properties[1] and structural transitions[2] that result from the lower-dimensional extended inorganic anions and the versatile organic cation layer which separates them. More recently, systems with the group 14 elements (Ge, Sn, and Pb) in the metal site have generated considerable interest for their conducting and luminescent properties.[3−11] A semiconductor−metal transition was found in the multilayer perovskites, $(C_4H_9NH_3)_2(CH_3NH_3)_{n-1}Sn_nI_{3n+1}$, as a function of increasing thickness of the perovskite sheets.[3] Intense room-temperature photoluminescence has also been observed in the Sn(II) and Pb(II) systems, at wavelengths ranging from the ultraviolet through the red spectral region. The ability to tune the wavelength through the choice of metal atom, halogen, or the thickness of the perovskite sheets has also been achieved.[6−9]

Recently, an electroluminescent device has been demonstrated, using $(C_6H_5C_2H_4NH_3)_2PbI_4$ as an emitter material, producing highly intense green luminescence of more than 10 000 cd m^{-2} (at liquid nitrogen temperature), with a current density of 2 A cm^{-2}.[10] The combination of the potentially useful optical and transport properties and the range of materials processing options, which include growing sizable single crystals from near-ambient temperature solutions,[3,8,9,12] and spin-coating[10] or thermal evaporation[11] of thin films, suggests that these materials might be attractive candidates for incorporation into light-emitting devices. Before this can happen, however, it is necessary to improve the room-temperature luminescent efficiency and to, more generally, gain a better understanding of this class of materials.

In this work, we report the first example of an organic−inorganic layered perovskite with a divalent rare-earth metal atom in the "M" site. Pellets of this compound can be made by a low-temperature (140−160 °C) solid-state reaction. The new compound produces intense blue photoluminescence at room temperature, with a peak wavelength of 460 nm and a fairly narrow peak width (fwhm = 24 nm). In contrast to $(C_4H_9NH_3)_2MI_4$ (M = Sn, Pb), for which mobile Wannier excitons radiatively decay to produce luminescence, the strong emission in $(C_4H_9NH_3)_2EuI_4$ arises from a more localized excitation between the Eu^{2+} ground state, $4f^7$, and the

* To whom correspondence should be addressed.

⊗ Abstract published in *Advance ACS Abstracts,* November 1, 1997.

(1) de Jongh, L. J.; Miedema, A. R. *Adv. Phys.* **1974**, *23*, 1. Dupas, A.; Le Dang, K.; Renard, J.-P.; Veillet, P.; Daoud, A.; Perret, R. *J. Chem. Phys.* **1976**, *65*, 4099. Estes, W. E.; Losee, D. B.; Hatfield, W. E. *J. Chem. Phys.* **1980**, *72*, 630. Willett, R. D.; Wong, R. J.; Numata, M. *Inorg. Chem.* **1983**, *22*, 3189. Bogdanov, A. N.; Zhuravlev, A. V.; Telepa, V. T. *Fiz. Nizk. Temp.* **1984**, *10*, 635. Zhou, P.; Drumheller, J. E.; Rubenacker, G. V.; Halvorson, K.; Willett, R. D. *J. Appl. Phys.* **1991**, *69*, 5804 and references therein.

(2) Needham, G. F.; Willett, R. D.; Franzen, H. F. *J. Phys. Chem.* **1984**, *88*, 674. Doudin, B.; Chapuis, G. *Acta Crystallogr.* **1990**, *B46*, 175 and references therein.

(3) Mitzi, D. B.; Feild, C. A.; Harrison, W. T. A.; Guloy, A. M. *Nature* **1994**, *369*, 467.

(4) Mitzi, D. B.; Wang, S.; Feild, C. A.; Chess, C. A.; Guloy, A. M. *Science* **1995**, *267*, 1473.

(5) Mitzi, D. B. *Bull. Am. Phys. Soc.* **1993**, *38*, 116.

(6) Papavassiliou, G. C.; Koutselas, I. B. *Synth. Met.* **1995**, *71*, 1713.

(7) Ishihara, T.; Takahashi, J.; Goto, T. *Phys. Rev. B* **1990**, *42*, 11099.

(8) Hong, X.; Ishihara, T.; Nurmikko, A. V. *Phys. Rev. B* **1992**, *45*, 6961.

(9) Mitzi, D. B. *Chem. Mater.* **1996**, *8*, 791.

(10) Era, M.; Morimoto, S.; Tsutsui, T.; Saito, S. *Appl. Phys. Lett.* **1994**, *65*, 676.

(11) Era, M.; Hattori, T.; Taira, T.; Tsutsui, T. *Chem. Mater.* **1997**, *9*, 8.

(12) Arend, H.; Huber, W.; Mischgofsky, F. H.; Richter-van Leeuwen, G. K. *J. Cryst. Growth* **1978**, *43*, 213.

S0897-4756(97)00352-9 CCC: $14.00

$4f^65d^1$ configurations. Examination of the title compound therefore provides an interesting opportunity to compare the luminescent properties for similar layered organic−inorganic perovskite structures with, however, a different degree of localization of the excitation giving rise to the luminescence.

Experimental Section

Sample Preparation and Characterization. Polycrystalline $(C_4H_9NH_3)_2EuI_4$ samples were prepared using a low-temperature solid-state reaction, with all synthetic steps and subsequent materials characterization being performed in an inert atmosphere. Stoichiometric amounts of europium(II) iodide (0.243 g, 0.6 mmol) and butylammonium iodide (0.241 g, 1.2 mmol) were weighed in an argon-filled drybox with oxygen and water levels maintained below 1 ppm. An intimate mixture of the two starting materials was pressed into pellets and subsequently placed into a quartz tube, which had been thoroughly dried by heating under vacuum before being brought into the drybox. In addition to the stoichiometric pellets, a few flakes (approximately 0.010 g) of additional $C_4H_9NH_2$·HI were also added to the reaction tube.

The conditions for the solid-state reaction were chosen based on differential thermal analysis (DTA) and thermogravimetric analysis (TGA) performed on similarly prepared mixtures of unreacted starting materials (see below). The reaction tube, containing an argon atmosphere, was sealed and placed into a preheated 140 °C tube furnace. After maintaining the temperature at 140 °C for 5 days, the temperature was raised to 150 °C for 4 days, and to 160 °C for 8 h, before finally being cooled over several hours. The initial weight of the pellets after pressing was 0.475(2) g, and after the heating cycle was 0.473(2) g, indicating that the overall composition of the pellets had not changed during the process. Infrared (IR) transmission spectroscopy, using KBr pellets containing the product, yielded the following major peaks (cm^{-1}): 903 m, 928 m, 1009 m, 1042 m, 1076 m, 1160 m, 1390 w, 1471 s, 1574 s, 2380 w, 2477 w, and a broad region of strong peaks, including 2874, 2931, 2962, 3050 (broad), 3168 (shoulder). The IR spectrum for the product was in good agreement with a spectrum taken for the starting material $C_4H_9NH_2$·HI, indicating that the organic cation remained intact after the heating cycle.

Thermal Analysis. Simultaneous thermogravimetric analysis (TGA) and differential thermal analysis (DTA) were performed, using a Seteram TAG 24 thermal analysis system, to examine the reactivity, thermal stability, and possible phase transitions in the title compound. Measurements were made both on an unreacted, stoichiometric (2:1) mixture of $C_4H_9NH_2$·HI and EuI_2, and on a sample of $(C_4H_9NH_3)_2EuI_4$ prepared as described above. In addition, the starting materials, $C_4H_9NH_2$·HI and EuI_2, were also examined separately. Approximately 40−90 mg of sample was loaded into a tantalum container for each run. The thermal cycling was performed using a 2 °C/min ramp rate in an argon atmosphere. Special care was taken to exclude oxygen from the apparatus by evacuating and back filling the thermal analysis setup with argon. The temperature was calibrated using the melting transitions of indium (T_m = 156.6 °C) and tin (T_m = 231.9 °C) using the same system configuration (crucible type, temperature ramp rate, gas type, gas flow, etc.).

X-ray Diffraction. Room-temperature X-ray powder diffraction patterns were collected for each batch of samples, using a Siemens D5000 diffractometer, and showed the products to be single phase. Since samples of $(C_4H_9NH_3)_2EuI_4$ degrade very rapidly in air, it was necessary to contain the sample in an airtight cell during the diffraction run. Regions of each data set were collected twice to ensure that the sample had not significantly degraded during the first scan.

All 30 of the observed peaks in the region $2° \le 2\theta \le 50°$ indexed to an orthorhombic unit cell with dimensions very similar to those observed for $(C_4H_9NH_3)_2MI_4$ (M = Ge, Sn, Pb). Of the 30 peaks, 28 were singly indexed (corresponded to one *h*,*k*,*l*), using an angular tolerance of 0.018°. The unit-cell dimensions were refined using the Siemens WIN-METRIC program (least-squares approach), after stripping the Cu $K\alpha_2$ component from the diffraction pattern, yielding a = 8.913(3) Å, b = 8.759(3) Å, and c = 27.793(6) Å.

For comparison, $(C_4H_9NH_3)_2PbI_4$ was also prepared using the same solid-state technique as for the europium analogue and examined using powder X-ray diffraction. Of the 48 peaks observed over the interval, $2° \le 2\theta \le 50°$, all indexed (with 44 singly indexed) to the orthorhombic unit cell, a = 8.886(2) Å, b = 8.698(2) Å, and c = 27.637(5) Å. Since the lead(II) compound is relatively air-stable, it was possible to collect the powder pattern without using the air-sensitive cell and to collect each data point over a longer interval, leading to less noise in the diffraction pattern than for the $(C_4H_9NH_3)_2EuI_4$ sample.

Magnetic Measurements. For the magnetic measurements, samples of $(C_4H_9NH_3)_2EuI_4$ were specially prepared by packing an intimate stoichiometric (2:1) mixture of $C_4H_9NH_2$·HI and EuI_2 into a quartz cup before the heating cycle, rather than by using a die to press pellets. This was done to avoid incorporating possible magnetic impurities from the metallic die. Besides this precaution, synthetic conditions were similar to that described in the Sample Preparation section.

Magnetic measurements were performed in a Quantum Design SQUID magnetometer over the temperature range 1.8−300 K. For each magnetic measurement, approximately 80 mg of sample was used, and the susceptibility was measured using an applied magnetic field of 50 Oe. The sample holder background susceptibility was measured and subtracted from the sample measurement (it was several orders of magnitude weaker than the sample signal). The core diamagnetism for the atoms in the title compound was also calculated and subtracted from the measured paramagnetism before determining the effective Eu magnetic moment.

Photoluminescence. Fluorescence emission spectra were recorded at room temperature on a Spex Fluorolog-2 spectrometer using the front-face geometry. Light from a xenon arc lamp was used as the excitation source after passing it through a SPEX 1680 0.22 m double spectrometer. The emitted fluorescence was also passed through a similar double spectrometer to a SPEX 1911F detector.

Spectra were recorded for solid samples of $(C_4H_9NH_3)_2EuI_4$ as well as for EuI_2 (as received from the manufacturer; Aldrich-APL, anhydrous, 99.9%). The solid samples were first ground into a fine powder and contained in an airtight cell with a quartz window. Each spectrum was collected several times to ensure that the sample did not significantly degrade over the course of the measurement.

Results and Discussion

Synthesis and Thermal Analysis. As a result of the organic component, which decomposes at relatively low temperatures (T > 250 °C), organic−inorganic perovskites are typically made using relatively low-temperature solution chemistry techniques. Single crystals of many of the A_2MX_4 materials, with for example M = Cd, Cu, Fe, Mn, Pd, Ge, Sn, or Pb, can be grown by slow cooling or evaporating a solution containing the organic ammonium halide and the metal halide, with some of the more common solvents including, water, various alcohols, acetone, hydrohalic acids, and *n*-methyl-2-pyrrolidone.[9,12] The solution chemistry of Eu^{2+}, however, is complicated by the fact that there is a strong tendency for solvent molecules to become tightly bound to the metal, thereby impeding the formation of the layered perovskites. In addition, Eu^{2+} is susceptible to oxidation and is therefore not stable in many solvents, at least for the relatively long periods of time or the range of temperatures required to grow high-quality crystals. Given the difficulties of solution chemistry, solid-state techniques are potentially useful and have already been used for the preparation of

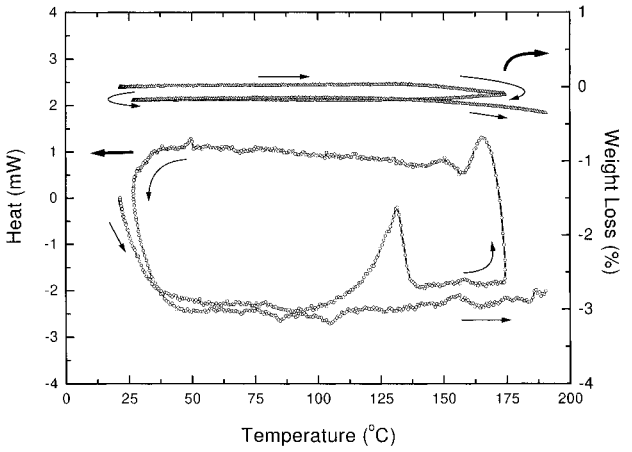

Figure 1. Simultaneous thermogravimetric analysis (TGA) and differential thermal analysis (DTA) scans for a previously unreacted stoichiometric (2:1) mixture of $C_4H_9NH_2$·HI and EuI_2. The temperature was ramped at 2 °C/min from 20 to 175 °C, back to 25 °C, and finally up to 190 °C, in an argon atmosphere.

inorganic Eu^{2+} ternary compounds. $AEuI_3$ (A = Cs, Rb) and AEu_2I_5 (A = K, Rb, Cs), for example, have been synthesized by the reaction of elemental Eu, AI (A = Cs, Rb), and HgI_2, in an evacuated sealed quartz tube.[13] However, this reaction occurs at temperatures up to 560 °C, conditions that would certainly lead to thermal decomposition of the organic cation in the case of the organic−inorganic perovskites.

We therefore first examined the direct solid-state reactivity of the organic ammonium iodide with EuI_2, using simultaneous differential thermal analysis (DTA) and thermogravimetric analysis (TGA), to determine whether a reaction would occur between the two components before the material decomposed. Figure 1 shows the DTA/TGA curves for an intimate stoichiometric (2:1) mixture of $C_4H_9NH_2$·HI and EuI_2. The temperature was ramped from room temperature to 175 °C, back to approximately 25 °C, and finally up to 190 °C, all in an argon atmosphere. Notice that during the first heating segment, there is a weak exotherm that begins around 100 °C and finishes by 140 °C. The exact temperature and width of this transition varied somewhat depending on how well the starting materials were ground and mixed and on how tightly they were packed into the tantalum crucible before heating, but in all cases the transition was completed by 160 °C. There is essentially no weight loss associated with this transition and the exotherm is not present during the second pass through this temperature range. Consequently, the low-temperature exotherm can be attributed to a reaction between the two starting materials. Further evidence of this can be deduced by a comparison with the thermal analysis curves for pure $C_4H_9NH_2$·HI (Figure 2a). The endotherm in this curve at 171(1) °C corresponds to the melting of the organic ammonium salt, before its bulk decomposition at temperatures above 250 °C. The absence of the endotherm in the DTA curve for the $C_4H_9NH_2$·HI/EuI_2 mixture during the second ramp up to 190 °C suggests that the $C_4H_9NH_2$·HI has reacted with EuI_2.

Figure 2b shows the thermal analysis curves for a section of a $(C_4H_9NH_3)_2EuI_4$ pellet, prepared at 160 °C

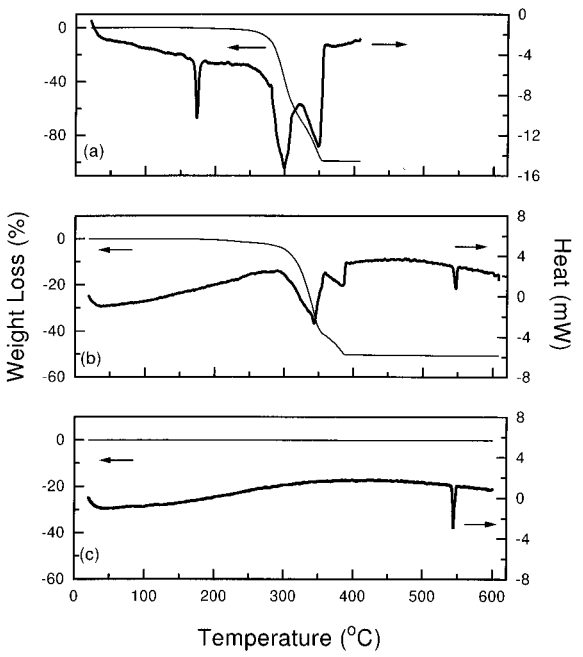

Figure 2. Simultaneous thermogravimetric analysis (TGA) and differential thermal analysis (DTA) scans for (a) $C_4H_9NH_2$·HI, (b) $(C_4H_9NH_3)_2EuI_4$ prepared by a solid-state reaction as described in the text, and (c) EuI_2. Each scan was performed in flowing argon with a ramp rate of 2 °C/min. For clarity, only the heating portions of the curves are shown.

as described in the Experimental Section. Notice that again there is no exotherm at low temperatures and no melting endotherm in the region 170−200 °C. There is also no sharp onset of weight loss as a function of temperature, but rather the material begins to slowly lose weight at temperatures as low as 150 °C, with bulk decomposition occurring around 290 °C. The weight loss during the decomposition corresponds to 50.3% of the initial weight. This is in good agreement with the expected weight loss (49.8%) for the complete loss of the organic component (in the form of $C_4H_9NH_2$·HI), leaving behind only the inorganic component of the compound, EuI_2. The endotherm at 543(1) °C therefore apparently corresponds to the melting of EuI_2, an assertion supported by the DTA curve for pure EuI_2 (Figure 2c), examined as received from the manufacturer (Aldrich-APL, anhydrous, 99.9%).

The thermal analysis curves for $(C_4H_9NH_3)_2EuI_4$ and the starting materials, $C_4H_9NH_2$·HI and EuI_2, demonstrate several useful points about the synthesis and thermal stability of the title compound. First, unlike $(C_4H_9NH_3)_2GeI_4$, for which it is possible to grow crystals from a stoichiometric melt,[9] melt processing cannot be used in this case (at least using a stoichiometric melt). Second, the study demonstrates that a solid-state reaction can be used to react $C_4H_9NH_2$·HI and EuI_2, without substantial decomposition. Since small weight losses are observed at relatively low temperatures in the TGA curves for $(C_4H_9NH_3)_2EuI_4$, the solid-state reaction is carried out in a sealed tube containing an inert atmosphere, rather than in an open system where the organic component can continuously leave the system. In addition, a small excess of $C_4H_9NH_2$·HI is included in the reaction tube, along with the stoichiometric $C_4H_9NH_2$·HI/EuI_2 pellets, to provide a partial pressure of $C_4H_9NH_2$ and HI in the ampule and therefore discourage the loss of the organic cation from the pellets. The

(13) Baopeng, C.; Shihua, W; Xinhua, Z. *J. Alloys Compd.* **1992**, *181*, 511. Wang, S. H.; Luo, S. M.; Eick, H. A. *J. Less-Common Met.* **1989**, *149*, 55.

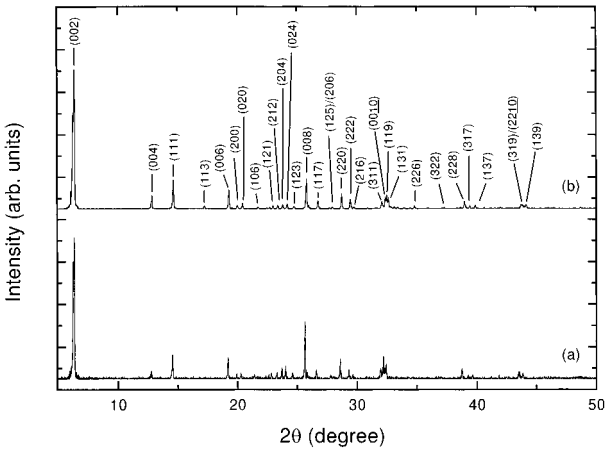

Figure 3. Room-temperature X-ray powder diffraction patterns for (a) $(C_4H_9NH_3)_2EuI_4$ and (b) $(C_4H_9NH_3)_2PbI_4$. Only the Cu $K\alpha_1$ component of the diffraction pattern is shown (i.e., the $K\alpha_2$ component has been stripped). While all reflections index to the orthorhombic lattice parameters given in the text, for clarity, only the reflection indices of the strongest peaks are indicated above the $(C_4H_9NH_3)_2PbI_4$ diffraction pattern. The reflection indexes are essentially identical for the two compounds, although more reflections are distinguishable for the lead(II) system, presumably because of the better signal-to-noise ratio for this spectrum.

fact that there is essentially no weight change observed for the pellets before and after the heating cycle verifies that these conditions fulfill their purpose.

Structural Aspects. Figure 3a shows the powder X-ray pattern for $(C_4H_9NH_3)_2EuI_4$, prepared by solid-state synthesis. The diffraction pattern is very similar to that observed for $(C_4H_9NH_3)_2PbI_4$ (Figure 3b), prepared using a similar solid-state reaction. For $(C_4H_9NH_3)_2EuI_4$, the refined orthorhombic lattice parameters are $a = 8.913(3)$ Å, $b = 8.759(3)$ Å, $c = 27.793(6)$ Å, compared with $a = 8.886(2)$ Å, $b = 8.698(2)$ Å, $c = 27.637(5)$ Å for the Pb(II) analogue. The very similar lattice constants, along with the virtually identical intensity ratios among the peaks of the diffraction patterns provide convincing evidence that the Eu(II) system adopts a layered perovskite structure analogous to that observed for the divalent Ge, Sn, and Pb halides.[9] These structures all consist of layers of corner-sharing MI_6 octahedra separated by bilayers of the butylammonium cations. The ammonium heads of the organic cations hydrogen/ionic bond to the metal halide sheets and the hydrocarbon tails extend into the space between the layers.

The refined orthorhombic lattice constants for $(C_4H_9NH_3)_2PbI_4$, prepared by solid-state synthesis, are similar to those previously reported for a single crystal of the lead(II)-based organic−inorganic perovskite, prepared by the slow cooling of an aqueous hydriodic acid solution ($a = 8.863(2)$ Å, $b = 8.682(1)$ Å, $c = 27.570(2)$ Å).[9] The slightly larger cell volume for the sample prepared by solid-state synthesis might be due to the higher temperatures used to prepare these samples, perhaps leading to vacancies in the organic cation site or to partial disordering of these cations in the structure. The single-crystal structures for the germanium(II) and tin(II) analogues have also been determined and have very similar orthorhombic layered perovskite structures with the lattice constants $a = 8.722(1)$ Å, $b = 8.272(1)$ Å, $c = 28.014(1)$ Å and $a = 8.837(1)$ Å, $b = 8.619(1)$ Å, $c = 27.562(2)$ Å, respectively.[9]

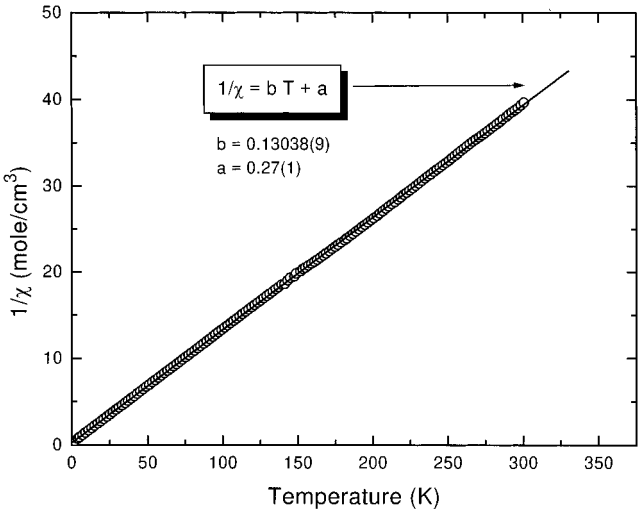

Figure 4. Inverse magnetic susceptibility as a function of temperature for $(C_4H_9NH_3)_2EuI_4$ in an applied field of 50 Oe. The weak diamagnetic signals from the sample holder and from the sample core diamagnetism have been subtracted from the observed paramagnetism. The fit of the observed data to a straight line is also shown, along with the refined coefficients *a* and *b*.

The 6-fold Eu(II) coordination in $(C_4H_9NH_3)_2EuI_4$ is similar to that observed in $CsEuI_3$, which adopts a three-dimensional distorted perovskite structure with the lattice constants $a = 8.624(2)$ Å, $b = 17.968(5)$ Å, $c = 12.540(3)$ Å.[13] This is in contrast to the situation for the room-temperature (and ambient pressure) phase of EuI_2, where an unusual 7-fold coordination is observed.[14] The *a* and *b* lattice parameters for $(C_4H_9NH_3)_2EuI_4$, which correspond to the values in the plane of the perovskite sheets, are approximately equal to $\sqrt{2}a_p$, where a_p is the lattice parameter for an ideal cubic perovskite. The average value for this parameter, derived from the two in-plane lattice constants, is $a_p = 6.248$ Å. By comparison, the orthorhombic lattice constants for $CsEuI_3$ approximately obey the relation $a = \sqrt{2}a_p$, $b = 2\sqrt{2}a_p$, $c = 2a_p$. The average value of a_p derived using this relation is $a_p = 6.240$ Å, a value very similar to that found in $(C_4H_9NH_3)_2EuI_4$. Notice that a_p, derived using this approach, does not necessarily yield exactly twice the Eu−I bond distance, as it would in a cubic perovskite, since the Eu−I−Eu bond angles between nearest-neighbor EuI_6 octahedra are not, in general, 180° (i.e., the octahedra can rotate to some degree relative to each other).

Magnetic Susceptibility. Magnetic measurements were undertaken for $(C_4H_9NH_3)_2EuI_4$ to examine the magnetic moment of europium in this material. Formally, europium should be present as Eu^{2+}, leading to a $^8S_{7/2}$ electronic ground state for the metal ion. Assuming that the europium ions are well isolated from each other (generally a very good assumption for rare-earth ions), Curie's law should apply with an expected paramagnetic moment close to the free-ion value of $\mu_{eff} = g\mu_b(J(J+1))^{1/2} = 7.94\mu_b$.

The inverse magnetic susceptibility of a sample of $(C_4H_9NH_3)_2EuI_4$ is shown as a function of temperature in Figure 4 and is approximately a straight line. The slope of the line yields the derived paramagnetic mo-

(14) Sanchez, J. P.; Friedt, J. M.; Bärnighausen, H.; van Duyneveldt, A. J. *Inorg. Chem.* **1985**, *24*, 408.

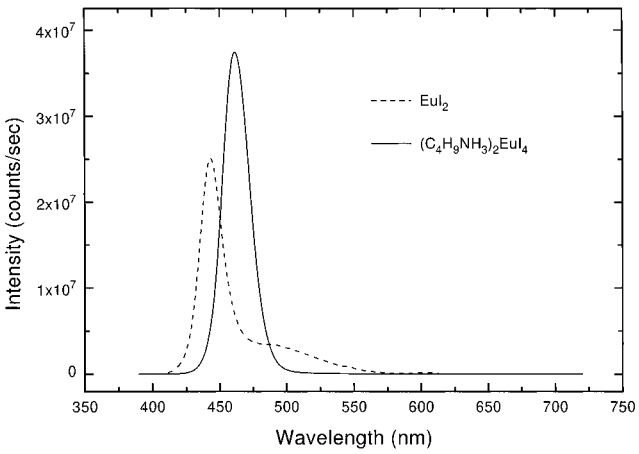

Figure 5. Room-temperature photoluminescence emission spectrum for ground solid-state samples of $(C_4H_9NH_3)_2EuI_4$ and EuI_2. The excitation wavelength for each spectrum was 370 nm.

ment for the europium ions, 7.8(1) μ_b, close to the predicted free-ion value and also very similar to the measured moments in EuI_2, $CsEuI_3$, and $RbEuI_3$.[14,15] The Curie temperature, θ, defined by $\chi = C/(T - \theta)$, is given by $\theta = -(a/b)$, where a and b are the coefficients of the straight-line fit of the inverse susceptibility versus temperature data (Figure 4). For the title compound we find $\theta = -2(1)$ K. The very small value for θ, as well as the absence of magnetic ordering at temperatures above 1.8 K, demonstrates the small degree of interaction between the europium moments. Note that within the europium dihalide family, $EuCl_2$ and EuI_2 order magnetically in a temperature range between 1.6 and 1.8 K, whereas $EuBr_2$ remains paramagnetic down to 1.1 K.[14] For the binary chalcogenides EuO, EuS, EuSe, and EuTe, the Curie temperature progressively decreases as the anion size increases (i.e., 79, 19, 8, and −4 K, respectively), as does the magnetic ordering temperature.[16]

Photoluminescence. Figure 5 shows the fluorescence emission spectra of powders of $(C_4H_9NH_3)_2EuI_4$ and EuI_2. EuI_2 emits at 442(1) nm, along with a shoulder that extends out to approximately 500 nm, in good agreement with published results.[17] $(C_4H_9NH_3)_2EuI_4$ powders give rise to a single, nearly symmetrical emission peak at 460(1) nm, a value which is red-shifted by approximately 18 nm relative to that for EuI_2. The emission peak full-width at half height is 24 nm, similar to that observed in the corresponding lead(II) iodide-based systems. The emission peak position appears to be relatively independent of excitation wavelength, although there is some variation in the intensity of the peak. The excitation spectrum (corresponding to the 460 nm emission) consists of several broad overlapping bands, ranging from a high-energy band centered at 275 nm, to one which extends from approximately 330 to 425 nm. The lower energy band is very broad and clearly has several components.

As in EuI_2, the emission of Eu^{2+} in the title compound is expected to result from the transition from the $4f^65d^1$ configuration to the ground state, 4f.[7] This assignment is based on the similar spectral characteristics between the present compound and EuI_2[17] and especially upon a comparison with the detailed measurements made on Eu^{2+} impurities in alkali halide hosts.[18] The 18 nm shift in the emission peak between EuI_2 and $(C_4H_9NH_3)_2EuI_4$ further supports the conclusion that the observed luminescence in these systems arises from a radiative transition involving the $4f^65d^1$ configuration. In contrast to transitions within the 4f manifold, which should be fairly independent of the local coordination, transitions involving the more extended 5d orbitals should result in more sensitivity to crystal field effects. In the Eu^{2+}-doped alkali iodides, for example, the emission peak shifts to the blue as the lattice parameter is increased by inserting larger alkali atoms.[18] The emission spectrum of EuI_2 has also been shown to depend on the structural details of the various high-pressure and ambient-pressure phases of this compound.[17] Similarly, the red shift between EuI_2 and $(C_4H_9NH_3)_2EuI_4$ most likely arises from the differences in local coordination. While Eu^{2+} sits at the center of an octahedra within $(C_4H_9NH_3)_2EuI_4$, it adopts an unusual 7-fold coordination within EuI_2.[14] It is also expected that the average Eu−I distance in the 7-fold coordinated compound should be longer than in the 6-fold coordinated compound.

In the lead(II)-based (as well as the tin(II)- and germanium(II)-based) organic−inorganic perovskites, luminescence arises from the radiative decay of free excitons associated with the two-dimensional inorganic sheets in the structure. In the purely inorganic PbI_2, the luminescence from the excitons is quenched at room temperature as a result of the small exciton binding energy (approximately 30 meV). In contrast, the exciton binding energies in the lead(II)-based organic−inorganic perovskites are on the order of 200−400 meV, enabling the strong photoluminescence associated with these excitons to be observed even at room temperature. The enhancement in binding energy is the result of the two-dimensionality of the structure, combined with an enhancement in the electron−hole coulomb interaction arising from the smaller dielectric constant for the organic layers that sandwich the metal halide sheets.[7,8]

In addition to the unusually strong binding energy, the effective dimensionality of the lead(II) halide sheets has a substantial impact on the wavelength at which luminescence is observed through a "quantum confinement effect". Specifically, as the thickness of the perovskite sheets increases (i.e., for example, by increasing n in the family $(C_{10}H_{21}NH_3)_2(CH_3NH_3)_{n-1}Pb_nI_{3n+1}$) the luminescence peak shifts to substantially longer wavelength,[6] ranging from 524 nm for $n = 1$ to 753 nm for the three-dimensional $n \rightarrow \infty$ compound (i.e., $CH_3NH_3PbI_3$). This fairly dramatic shift in the luminescence spectrum can readily be understood by a bandgap reduction with increasing perovskite sheet thickness and is the same effect that leads to a semiconductor−metal transition as a function of increasing perovskite sheet thickness in the family $(C_4H_9NH_3)_2(CH_3NH_3)_{n-1}Sn_nI_{3n+1}$.[3]

In contrast to the lead(II)- and tin(II)-based organic−inorganic perovskite families, the luminescence in the

(15) Shihua, W.; Qin, L.; Baopeng, C.; Xiaodong, W.; Xinhua, Z. *J. Alloys Compd.* **1992**, *181*, 515.

(16) Wachter, P. *Handbook on the Physics and Chemistry of Rare Earths*; Gschneidner, K. A., Jr., Eyring, L., Eds.; North-Holland Publishing Co.: Amsterdam, 1979; Vol. 2, Chapter 19, p 515.

(17) Wang, L.; Wang, S.; Zhao, X.; Sun, J. *J. Alloys Compd.* **1995**, *225*, 174.

(18) Hernandez A., J.; Lopez, F. J.; Murrieta S., H.; Rubio O., J. *J. Phys. Soc. Jpn.* **1981**, *50*, 225.

europium(II) compounds is less sensitive to global structural details. In the layered compound $(C_4H_9NH_3)_2EuI_4$ (i.e., $n = 1$), for example, the luminescence peak occurs at 460 nm, while for the three-dimensional system, $CsEuI_3$, the emission peaks at 449 nm.[19] Recently, we have also synthesized the $n \rightarrow \infty$ compound, $CH_3NH_3EuI_3$ (which adopts a tetragonally distorted perovskite structure similar to that observed in $CH_3NH_3PbI_3$ at room temperature) and observed a luminescent peak at approximately the same wavelength as for $CsEuI_3$ (i.e., 448(1) nm).[20] Consequently, the emission peaks for the europium(II) family occur at very similar wavelengths for the three-dimensional perovskites and the two-dimensional layered system. The small shift that is observed is in the direction opposite from that found in the lead(II)- and tin(II)-based families. This is presumably because of the different nature of the excitation giving rise to the luminescence in the two systems. Whereas in the lead(II), tin(II), and germanium(II) systems, the luminescence arises from the radiative decay of free excitons associated with the material's bandgap, the luminescence in the europium(II) system appears to arise from a more local excitation centered on the europium(II) ion, which is therefore less sensitive to the overall dimensionality of the structure.

The photoluminescence in $(C_4H_9NH_3)_2EuI_4$ is also found to be more robust than in $(C_4H_9NH_3)_2PbI_4$. For the lead(II) compound, strong green luminescence is observed at room temperature in well-crystallized single crystals, but virtually no luminescence is observed in poorly crystallized samples, in finely ground crystals, or in pressed pellets of the material prepared by solid-state synthesis. In contrast, the europium(II) samples luminesce very strongly even in fine powders made using the solid-state technique. Presumably, this is also because the electronic states responsible for the luminescence are more localized in the europium compound. In the lead(II) systems, the excitons are more free to diffuse to defects, which can act as nonradiative decay centers.

Conclusion

Synthesis of organic−inorganic layered perovskites containing Ln^{2+} (Ln = rare-earth metal) is hampered by strong solvent interactions with the Ln^{2+} ions and the tendency of these ions to be readily oxidized. In this work, a low-temperature solid-state reaction technique has been described for the synthesis of single-phase polycrystalline $(C_4H_9NH_3)_2EuI_4$ samples. The observation of strong blue photoluminescence, and a europium magnetic moment corresponding to 7.8(1) μ_b, demonstrates that europium is present as Eu^{2+} in the title compound. Furthermore, the new material has been shown to be relatively stable in an inert atmosphere up to approximately 290 °C, above which bulk decomposition occurs through the loss of the organic amine and HI.

While this report concentrates on the system $(C_4H_9NH_3)_2EuI_4$, the structural similarity between the title compound and the families, $(C_4H_9NH_3)_2MI_4$, where M = Ge, Sn, Pb, suggests that the mixed-metal solid solutions, $(C_4H_9NH_3)_2Eu_{1-x}M_xI_4$, may also be achievable using a similar procedure to that described for the pure europium(II) and lead(II) compounds. Examination of luminescence and conductivity in these "doped" systems is an interesting area of further study. In addition, among the rare-earth metals, europium has the smallest Ln^{3+}/Ln^{2+} oxidation potential, −0.34(1) V. After europium, the next element in the rare earth oxidation potential series is ytterbium, with a potential of −1.18(1) V, followed by samarium, −1.50(1) V, and thulium, −2.22(5) V.[21,22] It will be interesting to consider how far up the rare earth Ln^{3+}/Ln^{2+} redox series this solid-state technique can be applied for the formation of other organic−inorganic perovskites. While the conditions of synthesis are likely to get more stringent for the higher oxidation potential ions, there is also the potential for new organic−inorganic materials with interesting and potentially useful magnetic, luminescent, and conducting properties.

Acknowledgment. The authors gratefully acknowledge ARPA for partial support of this work under contract DAAL01-96-C-0095. In addition, the authors thank M. Prikas for technical assistance.

CM970352D

(19) Xinhua, Z.; Shihua, W.; Baopeng, C. *J. Alloys Compd.* **1992**, *180*, *235*.
(20) Mitzi, D. B., unpublished work, 1997.
(21) Morss, L. R.; McCue C. M. *Inorg. Chem.* **1975**, *14*, 1624.
(22) Mikheev, N. B.; Auerman, L. N.; Rumer, I. A. *Inorg. Chim. Acta* **1985**, *109*, 217.